

# Fabrication and magnetic properties of ordered $\text{Co}_{100-x}\text{Pb}_x$ nanowire arrays electrodeposited in AAO templates: Effects of annealing temperature and frequency

Mojgan Najafi<sup>a)</sup>

*Department of Materials Engineering, Hamedan University of Technology (HUT), Hamedan 65169-13733, Iran*

Pezhman Amjadi and Zahra Alemipour

*Department of Physics, University of Kurdistan, Sanandaj 66177-15175, Iran*

(Received 16 May 2016; accepted 9 February 2017)

$\text{Co}_x\text{Pb}_{1-x}$  nanowire arrays within an anodic aluminum oxide (AAO) template were electrodeposited from an appropriate acetate bath by applying alternating current (ac). The effect of the Pb content on magnetic properties of nanowire arrays was investigated. By adding  $\text{Pb}^{2+}$  to an electrolyte containing  $\text{Co}^{2+}$ , the coercivity field of nanowires decreased from 1508 Oe in  $\text{Co}_{100}$  to 921 Oe in  $\text{Co}_{92.5}\text{Pb}_{7.5}$  while squareness increased from 0.74 for Co nanowires to about 0.82 for  $\text{Co}_{92.5}\text{Pb}_{7.5}$  nanowire alloy sample. The effect of annealing on the magnetic properties of nanowires in the temperature range between 300 °C and 600 °C was also investigated. It was observed that the coercivity field of  $\text{Co}_{97.5}\text{Pb}_{2.5}$  nanowire increases from 1290 Oe at room temperature to 1785 Oe at 600 °C. Furthermore, the effect of electrodeposition frequency on the magnetic properties of  $\text{Co}_{97.5}\text{Pb}_{2.5}$  nanowires was studied. The coercivity was enhanced with increasing frequency; however, after annealing all samples exhibited enhanced coercivity regardless of the electrodeposition frequency.

## I. INTRODUCTION

Magnetic nanowire arrays have been investigated extensively due to their promising application. In particular, the fabrication of ordered magnetic nanowire arrays has attracted considerable scientific and commercial interest because of their potential application in magnetic recording.<sup>1,2</sup>

Among the fabrication methods reported for nanowire arrays, the template synthesis method, pioneered by Martin,<sup>3</sup> has proved to be an effective low-cost method with high yield. The nanoporous films which had been used contain polycarbonate films, nanochannel array glasses, mesoporous channel hosts, and anodic aluminum oxide (AAO) templates. Compared with other membranes, the AAO template has a number of useful characteristics such as self-organization, cylindrical shape, and uniformity. Moreover, the AAO templates contain holes parallel to each other and perpendicular to the surface whose dimensions can be readily controlled by adjusting the anodization conditions. The AAO template is also stable at high temperature.

A number of methods have also been used to synthesize the nanowire arrays, such as sputtering, chemical vapor

deposition, and molecular beam epitaxial techniques. Among these methods, electrodeposition is suitable for fabricating the arrays of magnetic nanowire using an AAO template.<sup>4–7</sup> High speed, low cost, and high efficiency filling are the main advantages of fabricating nanowires by electrodeposition on the AAO template.

Arrays of magnetic nanowires containing Fe, Co, Ni, and their alloys prepared based on the AAO template electrodeposition method exhibit interesting magnetic and transport properties.<sup>8–20</sup> Many nonmagnetic elements such as Cu,<sup>21</sup> Pd,<sup>22</sup> Pt,<sup>23,24</sup> and Pb<sup>25</sup> have been used as additives in the magnetic nanowire arrays to improve magnetic properties.

In the study of the magnetic nanowire arrays, magnetic–nonmagnetic alloys such as Co–Cu have been reported for the representation of particular magnetic characters.<sup>21,26</sup> Wang et al. have fabricated Fe–Ag and Co–Ag nanowire arrays embedded in an AAO template demonstrating the variation of the coercivities with changes in annealing temperature.<sup>27</sup> A few reports on Co–Pb alloys and more less than for Co–Pb nanowire alloys are available.<sup>25,28,29</sup> Up to now, there is still no report about the effect of electrodeposition frequency and  $\text{Co}^{2+}/\text{Pb}^{2+}$  ion concentration ratio on the magnetic properties and structures of electrodeposited Co–Pb nanowires.

In the present work, we report the measured magnetic properties of Co–Pb nanowire arrays by introducing different amounts of Pb in Co nanowires prepared by ac electrodeposition in a porous AAO template. The effects

Contributing Editor: Amit Goyal

<sup>a)</sup>Address all correspondence to this author.

e-mail: najafi@hut.ac.ir, mojgannajafi1@gmail.com

DOI: 10.1557/jmr.2017.67

of the annealing temperatures and electrodeposition frequencies on magnetic properties of nanowires have also been investigated. Scanning electronic microscopy (SEM), X-ray diffraction (XRD), energy-dispersive X-ray (EDX), and alternating gradient force magnetometer (AGFM) were used for the analysis of the prepared nanowires.

## II. EXPERIMENTAL

The AAO templates used for electrodeposition of Co<sub>x</sub>Pb<sub>100-x</sub> nanowire arrays were prepared using 99.99% pure aluminum foils via the two-step anodization process. Discs with thickness of 0.3 mm and diameters of 8 mm were degreased in acetone for 6 min and cleaned with deionized water. Then Al discs were annealed at 450 °C for 20 min in Ar atmosphere to remove structural disordering of aluminum. Subsequently, the oxide layer was detached by immersing the discs in a 3 mol/L NaOH solution for 5 min at room temperature. A mirror surface was then obtained by electropolishing in a 1:4 volume mixture of HClO<sub>4</sub> and C<sub>2</sub>H<sub>5</sub>OH at room temperature for 6 min. The ordered AAO templates were fabricated by the two-step anodizing process. In the first anodization step, Al discs were anodized in a 0.3 mol/L oxalic acid solution under a constant voltage of 40 V for 15 h at 15 °C. Then, the anodized layer was removed in a mixture of 0.2 mol/L chromic acid and 0.5 mol/L phosphoric acid at 70 °C for 15 h. The second anodization was performed under the same conditions as that of the first, for 1 h. To fabricate the nanowires through ac electrodeposition into the pores, it is necessary to reduce the barrier layer thickness at the pore bottom by systematically decreasing the anodization voltage from 40 V to 8 V in three steps. In the first step, the anodization voltage was reduced at a rate of 4 V/min to 20 V, and then at a rate of 2 V/min to 10 V, and finally at a rate of 1 V/min to 8 V. At the end of the third step, anodization was continued for 3 min at 8 V so that the barrier layer could reach its stable thickness. Lastly, Co–Pb alloy nanowires were electrodeposited within AAO pores. Electrodeposition was carried out by application of an ac sinusoidal voltage waveform (30 V<sub>pp</sub>, 200 Hz) at 15 °C for 4 min.

Preliminary experiments involving electrodeposition of Co–Pb nanowires at room temperature were performed with two different baths; a nitrate salt of Co and Pb was used in the first bath. The EDX analyses and measurement of the magnetic properties of the deposited nanowires indicated that only Pb ions were deposited and no Co co-deposition occurred. In the second experiment, acetate salts of Pb and Co ions were used for the preparation of nanowires. This is in agreement with the recently reported results by Péter et al. on co-electrodeposition of Pb and Co, showing that the co-electrodeposition of Pb and Co from nitrate bath is impossible given the lower redox potential of Pb than

that of Co.<sup>30</sup> They confirm that this interesting feature of the Co–Pb acetate bath was due to enclosing of the deposition and dissolution potentials of Co and Pb. Since only acetate bath could yield Co and Pb co-electrodeposition, all the nanowires were synthesized in the acetate bath.

The electrolyte solution for electrodeposition of Co–Pb nanowires contained  $x$  M Co(CH<sub>3</sub>COO)<sub>2</sub>·4H<sub>2</sub>O;  $y$  M Pb(CH<sub>3</sub>COO)<sub>2</sub>·3H<sub>2</sub>O, 30 g/L H<sub>3</sub>BO<sub>3</sub> with pH = 5.37. The percentage of Pb<sup>2+</sup> relative to that of Co<sup>2+</sup> in the electrolyte solution was selected as 0, 1, 2.5, 5, 6, and 7.5. During the electrodeposition, AAO template was chosen as a cathode electrode, and a Pt plate was chosen as an anode electrode. After electrodeposition, to study the effect of annealing on the magnetic properties, the Co–Pb nanowires were annealed for 20 min at various temperatures (300, 400, 450, 500, 550, and 600 °C) in an Ar atmosphere. Electrodeposition of all metals was carried out at room temperature.

The effect of electrodeposition frequency on the magnetic properties of the nanowires was investigated. To this end, the Co<sub>97.5</sub>Pb<sub>2.5</sub> nanowires were synthesized at various frequencies (50, 100, 200, 300, 400, 600, 800, 1000 Hz), particularly.

The magnetic properties were measured by an AGFM with the applied field parallel and perpendicular to the surface of the samples (maximum applied magnetic field was 9000 Oe). The morphology of the Co–Pb nanowires was observed by SEM and the chemical composition was determined by EDX. Furthermore, XRD has been used for determination of the crystalline structure of nanowire arrays. All electrodeposition of metals and magnetic measurements were carried out at room temperature.

## III. RESULTS AND DISCUSSIONS

Figure 1 shows the SEM images of the AAO template after first anodization. Figure 1(a) indicates the cross-sectional view, in which the cylindrical channels parallel to each other can be clearly seen. Figure 1(b) shows the top view of the AAO template. As is evident, the AAO template has an ordered structure of pores forming an array with an average diameter about 35 nm. Also, the SEM image of Co–Pb nanowires is shown in Fig. 2 after removal of the AAO template by dissolving in an aqueous solution of 5 M NaOH for 5 min. After each synthesis, nanowires were analyzed by EDX to determine the Co and Pb contents in nanowires. Figure 3 shows the at.% of Pb ingredient in electrodeposited Co–Pb nanowires at different concentrations of Pb<sup>2+</sup>( $x$ ) ions in the electrodeposition electrolyte (also, EDX spectra were shown as an inset). As indicated, the Pb content of the nanowire initially increased slowly with increasing Pb<sup>2+</sup> concentration and then varied with a steep slope increasing to

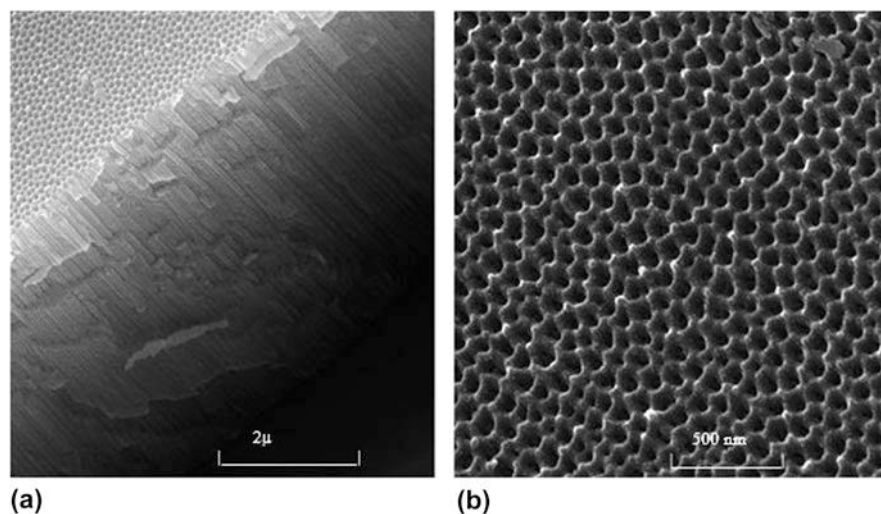


FIG. 1. SEM image of the anodic alumina oxide template with pores of 35 nm in diameter after first anodization: (a) the cross section view, (b) the top view.

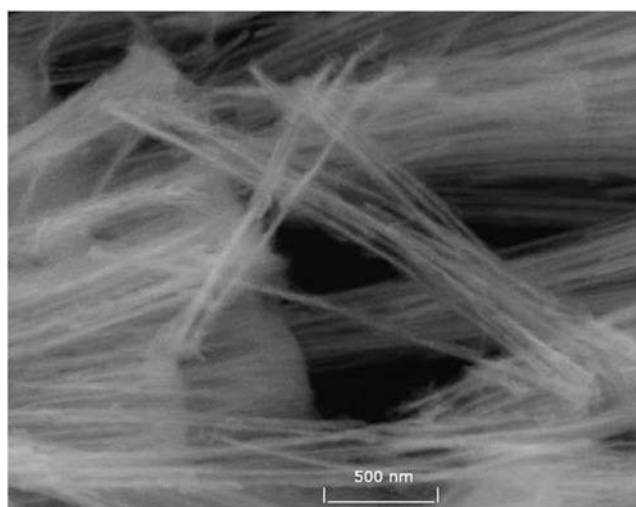


FIG. 2. SEM image of Co-Pb nanowires after removing of AAO template.

0.075 M  $\text{Pb}^{2+}$ . The changes in the at.% of nanowire ingredients with concentration of Co and Pb ions in the electrolyte are tabulated in Table I. During the electrodeposition process, a competition between Pb and Co exists and because of the larger redox potential value for  $\text{Pb}^{2+}$  as compared ( $-0.13$  V versus  $-0.28$  V for  $\text{Co}^{2+}$ ),  $\text{Pb}^{2+}$  ions were electrodeposited more extensively than Co. So it is expected that the Pb content of the nanowires will be larger than the Co content.

To investigate the magnetic properties of nanowires, magnetization and demagnetization of nanowires were measured using an AGFM. Hysteresis loops for each sample were plotted and magnetic parameters were extracted from the experimental data. Figure 4 illustrates the hysteresis curves corresponding to the external

magnetic field applied in parallel and perpendicular directions to the axis of typical as-deposited  $\text{Co}_{97.5}\text{Pb}_{2.5}$  nanowire arrays. It can be seen from this figure that the hysteresis curves are different in two directions. These different behaviors associated with the hysteresis loops demonstrate that the nanowires exhibit uniaxial anisotropy in which the easily magnetized axis is parallel to the nanowire's growth direction. The same results were obtained for all samples, indicating that shape anisotropy constitutes the main anisotropy in agreement with previous reports.<sup>31,32</sup>

The variation of coercivity and squareness with  $\text{Pb}^{2+}$  concentrations in the electrolyte is shown in Fig. 5. The results indicate that coercivity ( $H_c$ ) decreased from 1508 Oe to 921 Oe with increasing  $\text{Pb}^{2+}$  concentration in the electrolyte from 0% to 7.5% while the squareness ( $M_r/M_s$ ) increased from 0.74 to 0.82. This may be attributed to the replacement of some ferromagnetic Co atoms by nonmagnetic Pb atoms in the CoPb nanowires.

The hysteresis loops of Co and  $\text{Co}_{97.5}\text{Pb}_{2.5}$  nanowire arrays for the case in which the external magnetic field is parallel to the nanowire axis are compared in Fig. 6. As seen, the magnetization per surface area and coercivity have decreased by substitution of Co atoms with nonmagnetic Pb atoms.

By increasing the external magnetic field applied in parallel to the nanowire axis to 5000 Oe, the magnetization reversal was observed in Co and  $\text{Co}_{97.5}\text{Pb}_{2.5}$  samples. Both samples reach saturation magnetization ( $M_s$ ) however by scanning in the opposite direction, magnetization of Co nanowires decreases with decreasing the magnetic field, immediately; which the decrease in the magnetization of  $\text{Co}_{97.5}\text{Pb}_{2.5}$  nanowires was hindered in the magnetic field interval 5000 Oe to 2500 Oe. This may be due to the growth of Pb particles between Co particles (like pins)

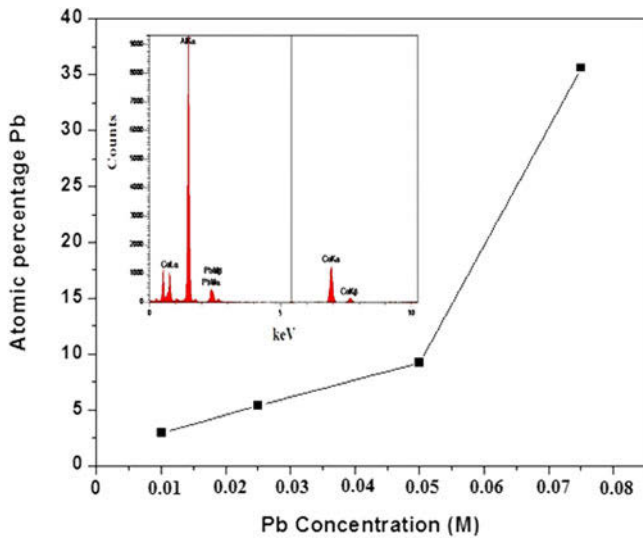


FIG. 3. Percentage atomic concentration of  $\text{Pb}(x)$  in electrodeposited  $\text{Co}_{100-x}\text{Pb}_x$  nanowires arrays versus the molar concentration of  $\text{Pb}$  in electrolyte obtained by EDX.

TABLE I. Pb atomic percent of Co–Pb nanowires as a function of  $\text{Co}^{2+}$  and  $\text{Pb}^{2+}$  concentrations in the electrolyte.

$\text{Co}^{2+}$ concentration (M)	$\text{Pb}^{2+}$ concentration (M)	Atomic percent of Pb	Atomic percent of Co
99	1	2.92	97.08
97.5	2.5	5.37	94.63
95	5	9.22	90.78
92.5	7.5	35.63	64.37

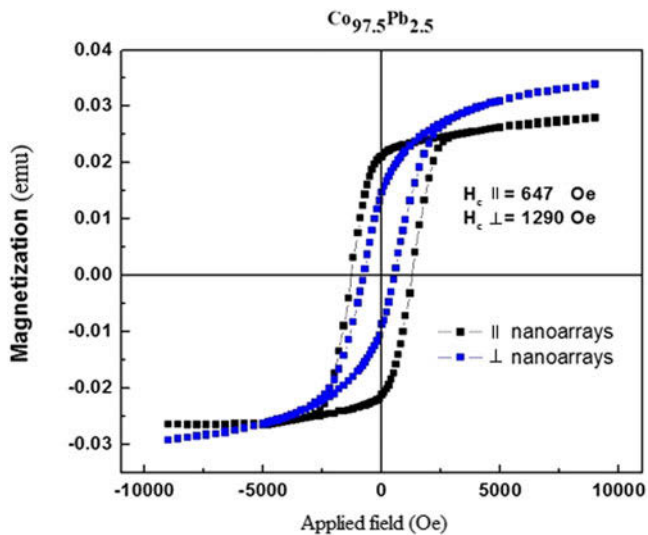


FIG. 4.  $M$ – $H$  loops of the as-deposited  $\text{Co}_{97.5}\text{Pb}_{2.5}$  nanowire arrays in an external magnetic field applied parallel and perpendicular to the axis of nanowires at room temperature.

hindering the rotation of the magnetization axis of saturation Co particles; therefore, squareness of  $\text{Co}_{97.5}\text{Pb}_{2.5}$  nanowires is higher than that of Co nanowires.

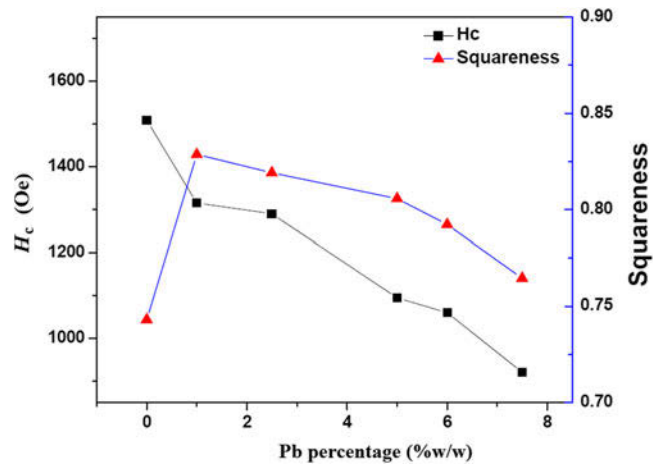


FIG. 5. Coercivity and squareness of Co–Pb nanowires as a function of Pb concentration in the electrolyte.

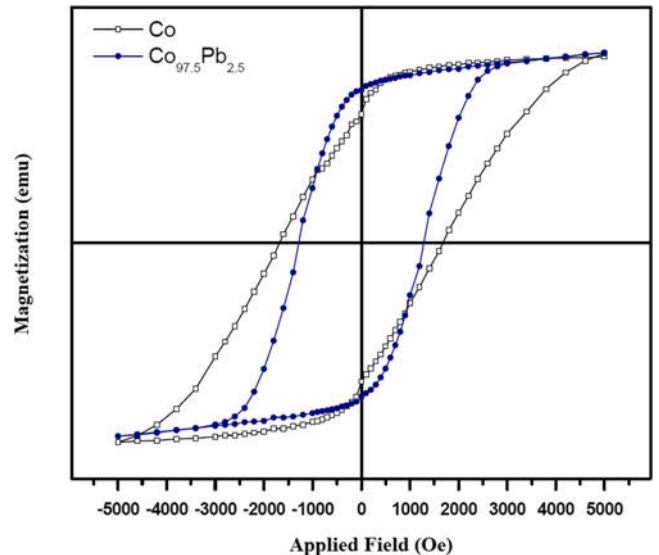


FIG. 6. Hysteresis loops of the Co and  $\text{Co}_{97.5}\text{Pb}_{2.5}$  nanowires arrays in a magnetic field parallel to the long axis of nanowires.

Co nanowires containing Pb, a nonmagnetic element, can exhibit a higher  $M_r/M_s$  ratio as compared with pure Co nanowires. As shown in Fig. 6, Pb–Co alloyed nanowires reach saturation at a field of 2500 Oe which is lower than that observed in pure Co nanowires.

To investigate the annealing effect on the magnetic properties of nanowires, all samples were annealed for 20 min at different temperatures (300, 400, 450, 500, 550 and 600 °C) in a flowing Ar atmosphere. The coercivity of annealed nanowires is shown in Fig. 7. The results demonstrate that the  $\text{Co}_{97.5}\text{Pb}_{2.5}$  nanowires show the largest variation in coercivity. Its coercivity is improved from 1290 Oe at room temperature to 1773 Oe at 600 °C.

According to Fig. 7, the coercivity of all samples increased with increasing the annealing temperature. The mechanism of this phenomenon can be explained

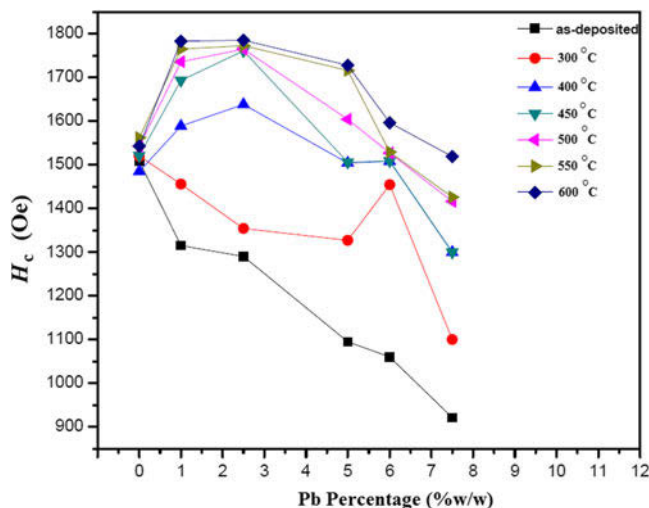


FIG. 7. Variation of coercivity of Co–Pb nanowires versus  $\text{Pb}^{2+}$  in bath composition at different temperatures.

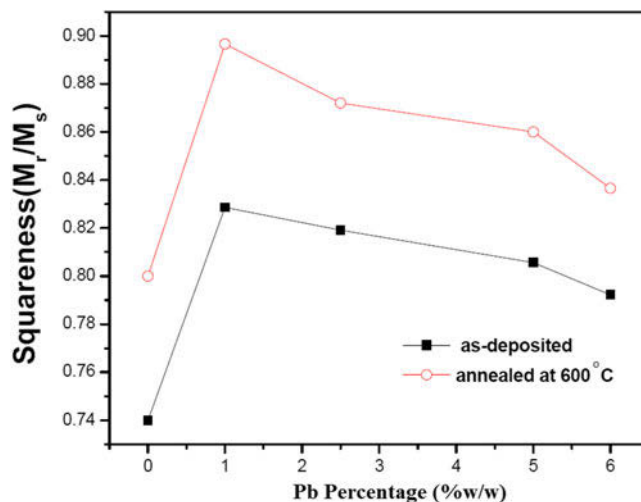


FIG. 8. Variation of  $M_r/M_s$  as-deposited Co–Pb nanowire arrays and after annealing at  $600\text{ }^\circ\text{C}$  versus  $\text{Pb}^{2+}$  concentrations.

based on high levels of intrinsic stress and defects in the as-deposited Co–Pb nanowires resulting from the rapid ac electrodeposition of Co and Pb in the AAO template.

The annealing treatment leads to an increase in the coercivity of nanowires as a result of structural relaxation and a reduction in defect levels.

On the other hand, after annealing, the Co–Pb nanowires showed a higher coercivity as compared with pure Co nanowires. Given the low value of the melting point for Pb, the Pb content is completely melted at the annealing temperature. The melted Pb should be capable of covering the small grains present in Co. Therefore, after solidification, the residual Pb may act like pins between Co grains as magnetic domain. The pins do not allow rotation of magnetization axis in Co nanowires during the magnetization reversal process. This, in turn, led to the higher coercivity and squareness of Co–Pb nanowires as compared with pure Co nanowires.

Figure 8 shows the squareness of the as-deposited and annealed samples at  $600\text{ }^\circ\text{C}$  versus  $\text{Pb}^{2+}$  concentrations in the electrodeposition bath. As is evident, the squareness of the annealed is higher than that of the as-deposited samples. This is due to the competition between the shape, stress, and magnetocrystalline anisotropies.<sup>33</sup> It is well known that the shape anisotropy may be slightly larger after thermal annealing at the annealing temperature above the crystallization temperature. At the very least, the stress anisotropy should not reduce the magnetic anisotropy along the longitudinal axis. Since the thermal expansion of Co–Pb alloy increases around the crystallization temperature, the external tensile stress caused by the thermal expansion mismatch between Co–Pb nanowires and AAO templates may increase and to be a positive value.

Figure 9 represents the XRD spectra pattern of the  $\text{Co}_{97.5}\text{Pb}_{2.5}$  nanowires before and after annealing at

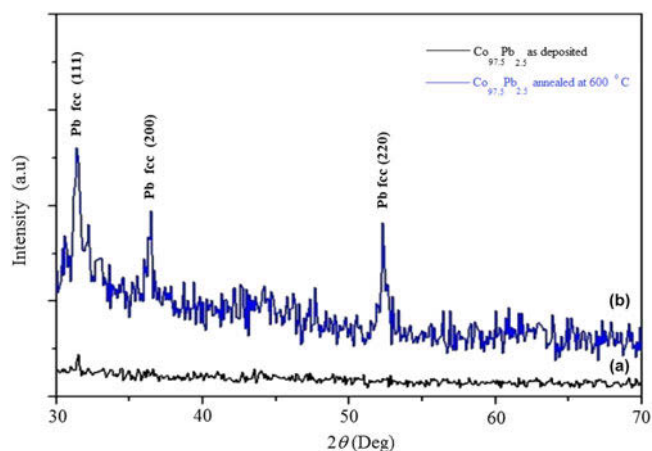


FIG. 9. The X-ray diffraction spectra of the  $\text{Co}_{97.5}\text{Pb}_{2.5}$  nanowires before annealing (a) and after Ar annealing at temperature  $600\text{ }^\circ\text{C}$  (b).

$600\text{ }^\circ\text{C}$ . The XRD pattern contains no diffraction peak for the as-deposited nanowire, indicating the presence of an amorphous structure. The XRD patterns demonstrate that the annealed samples are polycrystalline structure with peaks occurring in the planes (111), (200), and (220) in a face-centered-cubic (fcc) arrangement for Pb.

On the other hand, as the deposited nanowires transform from the amorphous phase into the crystalline phase, the magnetocrystalline anisotropy is strengthened drastically.

Neither the fcc nor the hexagonal-close-packed (hcp) structures were detected in the XRD spectra corresponding to Co peaks. This result may be attributed to the growth of the Co (as-deposited or after annealing) and Pb (as-deposited) grains that may be too small to be revealed by the XRD spectra. But during annealing and slow cooling in inert gas environment, Pb with a melting point



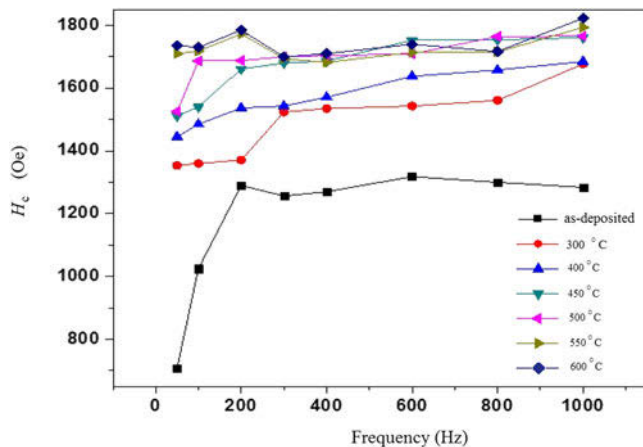


FIG. 10. The effect of frequency electrodeposition on magnetic properties optimized sample Pb 2.5%.

of 327.5 °C melted and crystallized in the fcc structure. Because of the large difference in the nearest neighbor distances for Co (0.25 nm) and for Pb (0.35 nm), it is expected not to crystallize Co and Pb in metastable alloy CoPb.

To consider the effect of electrodeposition frequency on the magnetic properties of the nanowires, the optimized sample (Pb 2.5% and Co 97.5%) was chosen and the samples were synthesized at different electrodeposition frequencies (50, 100, 200, 300, 400, 600, 800, 1000 Hz) and then annealed. Figure 10 shows the coercivity of  $\text{Co}_{97.5}\text{Pb}_{2.5}$  nanowires as a function of the electrodeposition frequency for as-deposited and annealed samples. As can be seen, with increasing frequency from 50 Hz to 200 Hz at room temperature, the coercivity increases from 708 Oe to 1295 Oe and after that with an increase in frequency from 200 Hz to 1000 Hz, the coercivity remains almost constant. Also, by increasing the annealing temperature, the coercivity of all samples increases slowly. The sample electrodeposited at 200 Hz shows the maximum coercivity after being annealed at 600 °C.

These results indicate that at lower frequencies, the rate of electrodeposition is faster. That is the presence of more defects on microstructures and internal stress leads to less coercivity at lower frequencies. By increasing the frequency more uniformly, deposition occurred.<sup>34</sup> It has also been confirmed that increasing the electrodeposition frequency causes a rotation of the easy axis from in-plane to being perpendicular to the plane of the samples, thereby increasing the coercive force.<sup>35</sup> The EDX analysis (not shown) revealed that the percentage of Co and Pb in synthesized nanowires was independent of frequency.

#### IV. CONCLUSION

$\text{Co}_{100-x}\text{Pb}_x$  ( $0 \leq x < 7.5$ ) nanowire arrays were fabricated by ac electrodeposition into AAO templates

in the presence of acetate  $\text{Co}^{2+}$  and  $\text{Pb}^{2+}$  anions, and the magnetic properties and microstructures of nanowires were also studied. The fabricated nanowires were about 35 nm in diameter and had relatively large aspect ratios (length-to-width ratio of 1000 or more).

The structure and magnetic properties of Co–Pb nanowires were influenced by the composition, the electrodeposition frequency, and the annealing temperature. The coercivity decreased with increasing the percentage of Pb in nanowires, but squareness of all alloys was more than that of pure Co nanowires. Also, after annealing, the greatest change in the coercivity for  $\text{Co}_{97.5}\text{Pb}_{2.5}$  was observed.

The structure of the nanowires was determined to be amorphous for Co and Co–Pb nanowires with Co–Pb crystallizing in the fcc structure after annealing.

The coercivity of  $\text{Co}_{97.5}\text{Pb}_{2.5}$  nanowires sample was also studied at various electrodeposition frequencies. The coercivity of prepared nanowires showed an increase as the frequency increased from 50 to 200 Hz reaching a constant value at 200 Hz.

On the other hand, the coercivity of samples was changed after annealing from the initial value of 708 Oe for the sample synthesized at 50 Hz and at room temperature to a high value of 1766 Oe that was prepared at 1000 Hz and 600 °C.

#### ACKNOWLEDGMENTS

The authors are grateful of the Grant Research Councils of HUT and Kurdistan Universities for the financial support.

#### REFERENCES

1. R.J. Tonucci, B.L. Justus, A.J. Campillo, and C.E. Ford: Nanochannel array glass. *Science* **258**, 783 (1992).
2. T.W. Whitney, J.S. Jiang, P.C. Searson, and C.L. Chien: Fabrication and magnetic properties of arrays of metallic nanowires. *Science* **261**, 1316 (1993).
3. C.R. Martin: Nanomaterials: A membrane-based synthetic approach. *Science* **266**, 1961 (1994).
4. B. Jaleh, A. Omidvar-Dezfuli, V. Jaberian-Hamedan, M. Najafi, and E. Tamari: The electrostatic potential at the center of associative magic squares. *Int. J. Phys. Sci.* **6**, 4775 (2011).
5. M. Najafi, S. Soltanian, H. Danyali, R. Hallaj, A. Salimi, S.M. Elahi, and P. Servati: Preparation of cobalt nanowires in porous aluminum oxide: Study of the effect of barrier layer. *J. Mater. Res.* **27**, 2382 (2012).
6. M. Koohbor, S. Soltanian, M. Najafi, and P. Servati: Fabrication of CoZn alloy nanowire arrays: Significant improvement in magnetic properties by annealing process. *Mater. Chem. Phys.* **131**, 728 (2012).
7. M. Najafi, P. Assari, A.A. Rafati, and M. Hamehvaisy: Effect of the electrodeposition frequency, wave form, and thermal annealing on magnetic properties of  $[\text{Co}_{0.975}\text{Cr}_{0.025}]_{0.99}\text{Cu}_{0.01}$  nanowire arrays. *J. Supercond. Novel Magn.* **27**, 2821 (2014).
8. M. Najafi, A.A. Rafati, M. Khorshidi Fart, and A. Zare: Effect of the pH and electrodeposition frequency on magnetic properties of binary  $\text{Co}_{1-x}\text{Sn}_x$  nanowire arrays. *J. Mater. Res.* **29**, 190 (2014).

9. M. Najafi, Z. Alemipour, I. Hasanzadeh, A. Aftabi, and S. Soltanian: Influence of annealing temperature, electrolyte concentration and electrodeposition conditions on magnetic properties of electrodeposited Co–Cr alloy nanowires. *J. Supercond. Novel Magn.* **28**, 95 (2015).
10. S.M. Hamidi, A. Sobhani, A. Aftabi, and M. Najafi: Optical and magneto-optical properties of aligned Ni nanowires embedded in polydimethylsiloxane. *J. Magn. Magn. Mater.* **374**, 139 (2015).
11. H. Moon, C. Nam, C. Kim, B. Kim, and G. Lee: Fabrication and characterization of iron–cobalt alloy magnetic nanocluster wires by thermal decomposition method in magnetic fields. *Mater. Res. Soc. Symp. Proc.* **776**, 119 (2003).
12. G. Sharma and C.A. Grimes: Synthesis, characterization, and magnetic properties of FeCoNi ternary alloy nanowire arrays. *J. Mater. Res.* **19**, 3695 (2004).
13. Y.V. Bhargava, S.A. Thorne, T.S. Mintz, T. Cohen Hyams, V. Radmilovic, Y. Suzuki, and T.M. Devine: Synthesis of magnetic self-assembled nickel-rich oxide nanowires using a novel electrochemical process. *Mater. Res. Soc. Symp. Proc.* **877**, 140 (2005).
14. N. Ahmad, J.Y. Chen, W.P. Zhou, D.P. Liu, and X.F. Han: Magnetoelastic anisotropy induced effects on field and temperature dependent magnetization reversal of Ni nanowires and nanotubes. *J. Supercond. Novel Magn.* **24**, 785 (2011).
15. X.Y. Zhang, G.H. Wen, Y.F. Chan, R.K. Zheng, X.X. Zhang, and N. Wang: Fabrication and magnetic properties of ultrathin Fe nanowire arrays. *Appl. Phys. Lett.* **83**, 3341 (2003).
16. B. Jaleh, F. Koosha, and A. Omidvar Dezfuli: Preparation and magnetic properties of Ni/Pd multilayer nanowire arrays. *J. Supercond. Novel Magn.* **27**, 1065 (2014).
17. J.C. Bao, Z. Xu, J.M. Hong, X. Ma, and Z.H. Lu: Fabrication of cobalt nanostructures with different shapes in alumina template. *Scr. Mater.* **50**, 19 (2004).
18. M.R. Tabasum, F. Zighem, J. De La Torre Medina, L. Piraux, and B. Nysten: Intrinsic switching field distribution of arrays of Ni<sub>80</sub>Fe<sub>20</sub> nanowires probed by *in situ* magnetic force microscopy. *J. Supercond. Novel Magn.* **26**, 1375 (2013).
19. S. Melle, J.L. Menendez, G. Armelles, D. Navas, M. Vazquez, K. Nielsch, R.B. Wehrspohn, and U. Gosele: Magneto-optical properties of nickel nanowire arrays. *Appl. Phys. Lett.* **83**, 4547 (2003).
20. L. Vlad, A.V. Sandu, and V. Georgescu: The Effects of the thermal treatment on the structural and magnetic properties of Zn–Co alloys prepared by electrochemical deposition. *J. Supercond. Novel Magn.* **25**, 469 (2012).
21. J. García, V.M. Prida, L.G. Vivas, B. Hernando, E.D. Barriga-Castro, R. Mendoza-Reséndez, C. Luna, J. Escrig, and M. Vázquez: Magnetization reversal dependence on effective magnetic anisotropy in electroplated Co–Cu nanowire arrays. *J. Mater. Chem. C* **3**, 4688 (2015).
22. X.L. Fei, S.L. Tang, R.L. Wang, H.L. Su, and Y.W. Du: Fabrication and magnetic properties of Fe–Pd nanowire arrays. *Solid State Commun.* **141**, 25 (2007).
23. T.R. Gao, L.F. Yin, C.S. Tian, M. Lub, H. Sang, and S.M. Zhou: Magnetic properties of CoPt alloy nanowire arrays in anodic alumina templates. *J. Magn. Magn. Mater.* **300**, 471 (2006).
24. X. Teng, M. Feyngenson, Q. Wang, J. He, W. Du, A.I. Frenkel, W. Han, and M. Aronson: Electronic and magnetic properties of ultrathin Au/Pt nanowires. *Nano Lett.* **9**, 3177 (2009).
25. G.B. Ji, S.L. Tang, B.X. Gu, and Y.W. Du: Ordered Co<sub>48</sub>Pb<sub>52</sub> nanowire arrays electrodeposited in the porous anodic alumina oxide template with enhanced coercivity. *J. Phys. Chem. B* **108**, 8862 (2004).
26. D. Reyes, N. Biziere, B. Warot-Fonrose, T. Wade, and C. Gatel: Magnetic configurations in Co/Cu multilayered nanowires: Evidence of structural and magnetic interplay. *Nano Lett.* **16**, 1230 (2016).
27. Y.W. Wang, L.D. Zhang, G.W. Meng, X.S. Peng, Y.X. Jin, and J. Zhang: Fabrication of ordered ferromagnetic–nonmagnetic alloy nanowire arrays and their magnetic property dependence on annealing temperature. *J. Phys. Chem. B* **106**, 2502 (2002).
28. G.B. Ji, W. Chen, S.L. Tang, B.X. Gu, Z. Li, and Y.W. Du: Fabrication and magnetic properties of ordered 20 nm Co–Pb nanowire arrays. *Solid State Commun.* **130**, 541 (2004).
29. G.B. Ji, S.L. Tang, W. Che, B.X. Gu, and Y.W. Du: Structure and magnetic properties of Co<sub>x</sub>Pb<sub>1-x</sub> nanowire arrays. *Solid State Commun.* **132**, 289 (2004).
30. K. Neuróhr, J. Dégi, L. Pogány, I. Bakonyi, D. Ungvári, K. Vad, J. Hák, A. Révész, and L. Péter: Composition, morphology and electrical transport properties of Co–Pb electrodeposits. *J. Alloys Compd.* **545**, 111 (2012).
31. S. Kumar and D. Saini: Large-scale synthesis of Au–Ni alloy nanowires using electrochemical deposition. *Appl. Nanosci.* **3**, 101 (2013).
32. L.F. Liu, S.S. Xie, and W.Y. Zhou: From Co/Pt multilayered nanowires to Co–Pt alloy nanowires: Structural and magnetic evolutions with annealing temperatures. *J. Phys. D: Appl. Phys.* **42**, 205002 (2009).
33. K. Maaz, S. Karim, M. Usman, A. Mumtaz, J. Liu, J.L. Duan, and M. Maqbool: Effect of crystallographic texture on magnetic characteristics of cobalt nanowires. *Nanoscale Res. Lett.* **5**, 1111 (2010).
34. A.J. Yin, J. Li, W. Jian, A.J. Bennett, and J.M. Xu: Fabrication of highly ordered metallic nanowire arrays by electrodeposition. *Appl. Phys. Lett.* **79**, 1039 (2001).
35. A. Ramazani, M. Almasi Kashi, M. Alikhani, and S. Erfanfam: Optimized microstructure and magnetic properties in arrays of ac electrodeposited Co nanowires induced by the continuous and pulse electrodeposition. *J. Phys. D: Appl. Phys.* **40**, 5533 (2007).